August 14, 2007

Surface Modification of Cetyltrimethylammonium Bromide-Capped Gold Nanorods to Make Molecular Probes

Chenxu Yu, *Purdue University*
Leo Varghese, *Purdue University*
Joseph Irudayaraj, *Purdue University*

Surface Modification of Cetyltrimethylammonium Bromide-Capped Gold Nanorods to Make Molecular Probes

Chenxu Yu, Leo Varghese, and Joseph Irudayaraj*

Department of Agricultural and Biological Engineering, Bindley Biosciences Center, Purdue University, 225 S. University Street, West Lafayette, Indiana 47907

Received April 16, 2007. In Final Form: May 30, 2007

A chemical procedure to replace the cetyltrimethylammonium bromide (CTAB) cap on gold nanorods (GNRs) fabricated through seed-mediated growth with organothiol compounds [3-animo-5-mercapto-1,2,4-triazole (AMTAZ) and 11-mercaptoundecaonic acid (MUDA)] was developed to reduce the cytotoxity of GNRs and facilitate further biofunctionalization. Compared to phosphatidylcholine (PC) modification, our procedure yields stable GNRs that are biocompatible and suitable for whole-cell studies. The PC-, AMTAZ-, and MUDA-activated GNRs all showed low cytotoxicity. By choosing different organothiols, net positive or negative charges could be created on the nanorod surface, for different applications. Gold nanorod molecular probes (GNrMPs) were fabricated by subsequent attachment of antibodies to the activated GNRs and were used to visualize and detect cell surface biomarkers in normal and transformed human breast epithelial cells, demonstrating the potential of developing novel biosensors using gold nanorods. The sensitivity of GNrMPs made from organothiol-activated GNRs is considerably higher than that of CTAB/PC-activated GNRs, demonstrating that the protocol reported here is favored in developing molecular probes using GNRs.

Introduction

Gold nanoparticles possess optical properties that render them suitable for sensing applications. Their optical properties strongly depend on both the particle size and shape and are related to the interaction between metal conduction electrons and the electric field component of the incident electromagnetic radiation, which leads to strong, characteristic absorption bands in the visible−NIR spectrum.[1]

In aqueous solutions, gold nanoparticles exhibit strong plasmonic bands according to their geometrical shape and size. The position and intensity of these bands can be affected by changes in the dielectric constant around the vicinity of the particle [known as nanoSPR[2] or localized surface plasmon resonance (LSPR)],[3] and this fact has been exploited for sensing applications.[2−10]

When nanostructures are used for optical sensing, nanorods are favored over spherical particles because of their distinct absorbance and pronounced spectral shift. Nanorods give rise to two absorption peaks corresponding to their plasmonic modes, transverse mode (∼520 nm) and longitudinal mode (usually ≥600 nm), corresponding to light absorption and scattering along the short and long axis, respectively.[1,11−14] The longitudinal band of the nanorods are more sensitive to changes in the dielectric constant around the vicinity of the particles than the transverse band absorption observed for spherical particles.

Since the mid-1990s, methods utilizing seed-mediated growth based on a wet chemistry approach were developed to synthesize gold nanorods, with controllable size and aspect ratio.[15−25] In these processes the presence of a structure-directing surfactant was crucial to obtaining a high percentage of nanorods. Cetyltrimethylammonium bromide (CTAB) has been found to be uniquely suited toward the synthesis of nanorods and is widely used.[15−25] CTAB selectively forms a tightly packed bilayer on the side faces of nanorods, which leaves the ends of the rods more exposed to facilitate anisotropic growth along the longitudinal axis. Further, CTAB-passivated nanorods are positively charged, and their mutual repulsion prevents aggregation so that the solution is in a stable form. However, the presence of CTAB poses two major obstacles in utilizing gold nanorods for biological applications. First, the tightly packed CTAB bilayer at the side faces of the gold nanorods is not conducive for biological functionalization, and second, CTAB is a cationic detergent and shows high cytotoxity at the fabricated concentrations (∼0.1

* Corresponding author. E-mail: josephi@purdue.edu.

(1) Perez-Juste, J.; Pastoriza-Santos, I.; Liz-Marz'an, L. M.; Mulvaney, P. *Coord. Chem. Rev.* **2005**, *249*, 1870.
(2) Nath, N.; Chilkoti, A. *J. Fluorescence* **2004**, *14*, 377.
(3) Haes, A.; van Duyne, R. P. *J. Am. Chem. Soc.* **2002**, *124*, 10596−10604.
(4) Nath, N.; Chilkoti, A. *Anal. Chem.* **2002**, *74*, 504.
(5) Yonzon, C. R.; Jeoung, E.; Zou, S.; Schatz, G. C.; Mrksich, M.; Van, Duyne, R. P. *J. Am. Chem. Soc.* **2004**, *126*, 12669.
(6) Ghosh, S. K.; Nath, S.; Kundu, S.; Esumi, K.; Pal, T. *J. Phys. Chem. B* **2004**, *108*, 13963.
(7) Dahlin, A.; Zach, M.; Rindzevicius, T.; Kall, M.; Sutherland, D. S.; Hook, F. *J. Am. Chem. Soc.* **2005**, *127*, 5043.
(8) Raschke, G.; Kowarik, S.; Franzl, T.; Sonnichscen, C.; Klar, T. A.; Feldmann, J.; Nichtl, A.; Kurzinger, K. *Nano Lett.* **2003**, *3*, 935.
(9) Raschke, G.; Brogl, S.; Susha, A. S.; Rogach, A. L.; Klar, T. A.; Feldmann, J.; Fieres, B.; Petkov, N.; Bein, T.; Nichtl, A.; Kurzinger, K. *Nano Lett.* **2004**, *4*, 1853.
(10) Lee, S.; Perez-Luna, H. *Anal. Chem.* **2005**, *77*, 7204.
(11) . Murphy, C. J.; Sau, T. K.; Gole, A. M.; Orendorff, C. J.; Gao, J.; Gou, L.; Hunyadi, S. E.; Li, T. *J. Phys. Chem.* **2005**, *109*, 13857.
(12) Hornyak, G. L.; Patrissi, C. J.; Martin, C. R. *J. Phys. Chem. B* **1997**, *101*, 1548.
(13) Kelly, K. L.; Coronado, E.; Zhao, L. L.; Schatz, G. C. *J. Phys. Chem. B* **2003**, *107*, 668.
(14) Sosa, I. O.; Noguez, C.; Barrera, R. G. *J. Phys. Chem. B* **2003**, *107*, 6269.
(15) Yu, Y.-Y.; Chang, E.-S.; Lee, C.-L.; Wang, C. R. C. *J. Phys. Chem. B* **1997**, *101*, 6661.
(16) Hu, J.; Odom, T. W.; Lieber, C. M. *Acc. Chem. Res.* **1999**, *32*, 435.
(17) Jana, N. R.; Gearheart, L. A.; Murphy, C. J. *Chem. Commun.* **2001**, 617−618.
(18) Jana, N. R.; Gearheart, L.; Murphy, C. J. *J. Phys. Chem. B* **2001**, *105*, 4065.
(19) Murphy, C. J.; Jana, N. R. *Adv. Mater.* **2002**, *14*, 80.
(20) Sun, Y.; Mayers, D.; Herricks, T.; Xia, Y. *Nano Lett.* **2003**, *3*, 955.
(21) Nikoobakht, B.; El-Sayed, M. A. *Chem. Mater.* **2003**, *15*, 1957.
(22) Liu, M.; Guyot-Sionnest, P. *J. Phys. Chem. B* **2004**, *108*, 5882.
(23) Sau, T. K.; Murphy, C. J. *Langmuir* **2004**, *20*, 6416.
(24) Walter, E. C.; Murray, B. J.; Favier, F.; Kaltenpoth, G.; Grunze, M.; Penner, R. M. *J. Phys. Chem. B* **2002**, *106*, 11407.
(25) Filankembo, A.; Giorgio, S.; Lisiecki, I.; Pileni, M.-P. *J. Phys. Chem. B* **2003**, *107*, 7492.

10.1021/la701111e CCC: $37.00
Published on Web 07/17/2007

M).[26−28] It has been reported that the cytotoxicity is not due to the nanorod-bound CTAB layer, but due to the excess CTAB left in the solution,[26] which can be removed by centrifugation. However, the CTAB bilayer is physisorbed onto the nanorods surface and constitutes a dynamic structure. Thus, even if it were possible to remove all of the unbound CTAB from the nanorod solution, some CTAB would eventually enter the solution from the nanorods' surfaces. Furthermore, removal of the desorbed CTAB will result in aggregation of the nanorods, because of the lack of a repulsive interaction between the individual particles. Thus, activation of gold nanorods (replacing the CTAB with biocompatible and functionalization-friendly stabilizing agents) is essential for the realization of functional nanorod probes that can be used in tissues and living cell studies.

Yamada and co-workers[29] have proposed a method in which CTAB on the gold nanorods was replaced by phosphatidylcholine (PC) through a chloroform-phase extraction procedure. The cytotoxicity of the PC-capped gold nanorods was shown to be low compared to the twice-centrifuged CTAB-capped gold nanorods. However, the PC layer is also a physisorbed layer, which is dynamic and less stable. To further facilitate the chemical modification for biosensing purposes a chemically bound linker layer is preferred.

Recently Pierrat and co-workers[30] reported a surface modification procedure using thiolated poly(ethylene glycol) (PEG) to replace CTAB. In this approach, the thiolated PEG was chemically bound to the gold nanorod surface to offer better stability compared to the PC approach. However, thiolated PEGs are polymers, much bigger in size compared to its smaller counterparts such as the PC, and the PEG coating creates a thicker layer than the PC layer. Since the plasmonic electromagnetic field surrounding the gold nanorod probe decays exponentially from the surface, when PEG-capped nanorods are used, bioactive agents are further away from the gold surface, and the nanorods become less sensitive to surface-binding events constituting these agents. Thus, the probe will suffer a loss in sensitivity. To synthesize highly sensitive molecular probes, smaller linker molecules are more desirable in the activation step.

The most commonly used activation method for a gold surface is the formation of a self-assembled monolayer (SAM) of alkanethiols at the surface. However, when alkanethiol−CTAB ligand exchange was directly used in activating CTAB-capped gold nanorods, the densely packed CTAB on the side faces of the gold nanorods obstructs the access of alkanethiol molecules to the gold surface, and only at the more exposed ends would the alkanethiols replace the CTAB. Therefore, only partial activation is accomplished and the CTAB bilayer on the side faces remains intact.[31−33]

In this paper, a new method is reported to completely replace the CTAB layer on gold nanorods with small, organothiol compounds. In order to provide the activated gold nanorods, a net positive or negative charge at the surface for different applications, with organothiols 3-animo-5-mercapto-1,2,4-triazole (AMTAZ) and 11-mercaptoundecaonic acid (MUDA), was used. The molecular structures of these two compounds are shown in Figure 1. For AMTAZ, the 5-mercapto groups of AMTAZ show strong affinity for gold; the 3-animo groups of AMTAZ ionized in aqueous solution produces a positively charged cap that maintains the stability of the nanorods in aqueous environment. For MUDA, the carboxylic groups are negatively charged in aqueous solutions and give the nanorod a negatively charged cap. Further the amino-/carboxylic-terminated gold nanorods can be modified for biologically relevant studies.

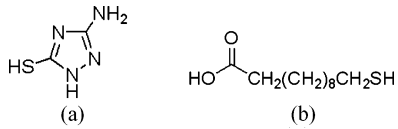

Figure 1. Molecular structures of the two organothiols used for GNR functionalization: (a) 5-mercapto-3-animo-1,2,4-triazole and (b) 11-mercaptoundecanoic acid.

Different applications require different surface modification strategy. It has been reported that positively charged gold nanoparticles can be uptaken by cells much more easily and efficiently than negatively charged gold nanoparticles;[32] therefore, for intracellular probing applications, amino-terminated gold nanorods are favored over carboxylic-terminated ones. On the other hand, most antibodies are negatively charged under physiological pH, when functionalizing carboxylic-terminated gold nanorods with antibodies to make molecular probes, the net negative charge on carboxylic-terminated nanorods will minimize physisorption due to electrostatic repulsion to yield better control over antibody coverage on a per-rod basis for quantitative assay development. In this paper, we demonstrate that both AMTAZ and MUDA modification could be achieved following a simple procedure to yield highly sensitive gold nanorod molecular probes.

Experimental Section

A seed-mediated growth procedure modified from that suggested by Nikoobakht and El-Sayed[21] was used to fabricate gold nanorods in the aspect ratio between 2.5 and 7. Details of the procedure were reported elsewhere.[34] Hexadecyltrimethylammoniumbromide (C_{16}-TAB, 99%), benzyldimethylammoniumchloride hydrate (BDAC, 99%), sodium borohydride (99%), L-ascorbic acid, gold(III) chloride hydrate (>99%), and silver nitrate (>99%) were all purchased from Sigma-Aldrich (St. Louis, MO) and used without further purification. Nanopure deionized and distilled water (18.2 MΩ) was used for all experiments. The concentration of atomic gold in the gold nanorod solution was determined by inductively coupled plasmon atomic emission spectroscopy (ICP-AES). Comparison of the concentration of atomic gold in the nanorod solution to the average nanorod volume obtained by TEM analysis yielded a molar concentration value in the range between 10 and 30 nM for gold nanorods of different aspect ratios. The gold nanorods were then concentrated to 100 nM by centrifugation. All subsequent characterization, activation, and functionalization steps were conducted using these nanorod samples.

Absorption spectra of GNrMP samples at every stage of the experimentation were measured using a Jasco V570 UV−vis−NIR spectrophotometer (Jasco, Inc., Easton, MD), in the wavelength range between 400 and 1500 nm. The measured spectra were normalized by rescaling the maximum absorbance of the longitudinal plasmon peak to 1.

Three different activation procedures were conducted to replace the CTAB cap with PC, AMTAZ, and MUDA, respectively. Three tubes of 10 mL of CTAB-capped gold nanorod solution were centrifuged at 3000 rpm for 15 min, the supernatant was disposed, and the nanorods were resuspend in three tubes of 10 mL of distilled

(26) Connor, E. E.; Mwamuka, J.; Gole, A.; Murphy, C. J.; Wyatt, M. D. *Small* **2005**, *1*, 325.
(27) Cortesi, R.; Esposito, E.; Menegatti, E.; Gambari, R.; Nastruzzi, C. *Int. J. Pharm.* **1996**, *139*, 69.
(28) Mirska, D.; Schirmer, K.; Funari, S. S.; Langner, A.; Dobner, B.; Brezesinski, G. *Colloids Surf. B* **2005**, *40*, 51.
(29) Takahashi, H.; Niidome, Y.; Niidone, T.; Kaneko, K.; Kawasaki, H.; Yamada, S. *Langmuir* **2006**, *22*, 2.
(30) Pierrat, S.; Zins, I.; Breivogel, A.; Sonnichsen, C. *Nano Lett.* **2007**, *7*, 259−263.
(31) Chang, J.; Wu, H.; Chen, H.; Ling, Y.; Tan, W. *Chem. Commun.* **2005**, 1092
(32) Caswell, K. K.; Wilson, J. N.; Bunz, U. H. F.; Murphy, C. J. *J. Am. Chem. Soc.* **2003**, *125*, 13914.
(33) Thomas, K. G.; Barazzouk, S.; Ipe, B. I.; Shibu, J. S. T.; Kamat, P. V. *J. Phys. Chem. B* **2004**, *108*, 13066.
(34) Yu, C.; Irudayaraj, J. *Anal. Chem.* **2007**, *7*, 572−579.

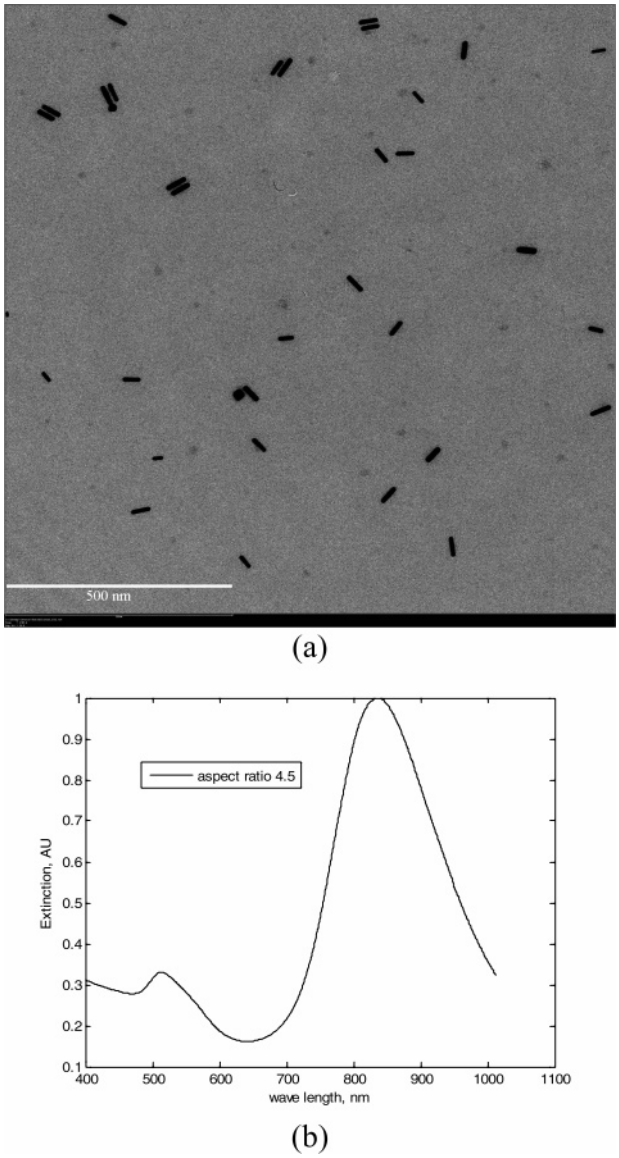

Figure 2. Typical GNRs made through seed-mediated growth, aspect ratio 4.5: (a) TEM image and (b) plasmon spectrum.

and deionized water. For PC activation, three rounds of extraction using 10 mL of 10 mg/mL PC (from egg yolk, Avanti Polar Lipids, Inc., Alabaster, AL) in chloroform (PC-chloroform) was conducted for 5 mL of the CTAB-capped GNR solution. The solution was then centrifuged at 5800 rpm for 5 min, the GNRs were collected and resuspended in 5 mL of pure water, and UV−vis−NIR spectra of the GNR solution were acquired. For AMTAZ/MUDA activation, the GNR solution was centrifuged one more time at 300 rpm for 15 min, and then 10 mL of 1 mM AMTAZ (Sigma-Aldrich Inc., St. Louis, MO) solution/1 mL of 20 mM MUDA−ethanol solution (Sigma-Aldrich Inc., St. Louis, MO) and 5 mL of pure water were added to resuspend the GNRs. Temperature was then elevated to 50 °C, the solution was kept under constant sonication for 30 min, the temperature was finally brought back to 25 °C, and the solution was kept under constant sonication for 2 h. The solution was then centrifuged at 5800 rpm for 5 min, the GNRs were collected and resuspended in 10 mL of pure water, and the UV−vis−NIR spectra were acquired.

In this procedure, control of reaction conditions is the key to the success of the activation. Temperature needs to be elevated to drive CTAB molecules to leave the GNR surface; however, if the temperature rises too fast, the exposed GNRs tend to aggregate; sonication will keep the aggregation from occurring, but at the same time, it also causes the CTAB to form small, micron-sized micelles

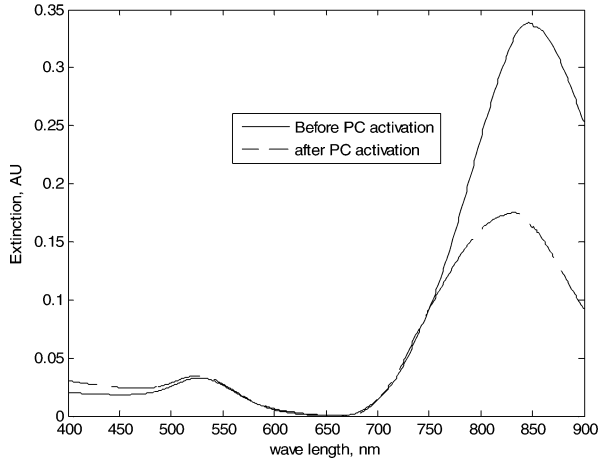

Figure 3. Plasmon spectra of GNRs before/after the CTAB−PC replacement.

that will interfere with the optical spectral measurement. The amount of the AMTAZ/MUDA−ethanol solution added also has an impact on the stability of GNRs. Through experimentation we have found that a temperature range of 45−50 °C, a sonication time of 30 min, and a AMTAZ/MUDA:GNR ratio of 500−600:1 produced fully activated stable GNRs.

After activation, the GNRs were further functionalized with antibodies to yield molecular probes. For the PC-activated GNRs, an appropriate chemical functionalization procedure was not readily available; antibody functionalization is simply done by incubating antibodies (100 μg/mL) with the PC−GNRs at room temperature. Antibodies were physisorbed onto the PC-based GNRs through nonspecific electrostatic interactions between charged side chains of antibodies and the charged P^- and N^+ groups of the PCs; for MUDA/AMTAZ-activated GNRs, a EDC-NHS mediated coupling procedure was used to attach the antibodies covalently, as discussed.[34]

Results and Discussion

A TEM image and plasmon spectra of the CTAB-capped gold nanorods are shown in Figure 2a,b. These nanorods have an average aspect ratio of 4.5, with length 32 ± 2 nm and width 7 ± 1.8 nm. The CTAB-capped GNRs were stable in the original, high-CTAB content solution for over 100 days; however, if CTAB was removed from the solution through centrifugation, the GNRs become unstable and start to aggregate.

For PC-activated nanorods, the recovery after three extraction cycles was quite low, yielding 30−40% with a major part of the nanorods being lost due to aggregation, suggesting that the PC−CTAB replacement is not very effective. This is demonstrated by the decrease in the plasmon band intensities before/after the CTAB−PC replacement, as shown in Figure 3. Because the volume of the GNR solution stayed the same, the concentration change, which is directly correlated to the intensity of the plasmon bands, reflects change in the number of individual GNRs in the solution. The decrease in the intensity of the longitudinal band by 50% suggests a major loss of GNRs harvested from this fabrication step, a key drawback of the PC activation procedure.

The wavelength of the plasmon bands of GNRs depends on the microenvironment of these rods. The dielectric properties of the medium surrounding the GNRs change during activation when the CTAB cap is replaced by another substance (PC, AMATZ, MUDA). Quantitatively, the response of the GNRs to changes in their surrounding microenvironment could be evaluated through the effective refractive index, which is defined by

$$n_{\text{eff}} = \frac{2}{l_d}\int_0^{\infty} n(z)\, E^2(z)\, \mathrm{d}z \qquad (1)$$

where

$$n(z) = \begin{cases} n_{cap}, 0 \le z \le d_{\text{cap}} \\ n_{\text{water}}, d_{\text{cap}} \le z < \infty \end{cases}$$

Here n_{cap} is the refractive indexes of the cap material, i.e., CTAB, PC, AMATZ, and MUDA, and n_{water} denotes the refractive indexes of water, which is 1.33. $E(z)$ is assumed to be only dependent on the local surface normal z, and l_d is the characteristic decay length. The factor $2/l_d$ normalizes the integral in eq 1 so that $n_{\text{eff}} = n_{\text{water}}$ when $n(z) = n_{\text{water}}$ for all z. Exponential decay for $E(z)$ was assumed in this work, $E(z) = \exp(-z/l_d)$, with $l_d \sim 5-6$ nm, which was consistent for a saturation distance of $\sim$30 nm.[35]

The effective refractive index for CTAB and PC caps could be calculated, $n_{\text{CTAB}} = 1.435$ [36] and $n_{\text{PC}} = 1.42$,[37] and the thickness of the CTAB and PC caps, which are both bilayer structures, are 4−5 nm.[36] Using these parameters, the effective refractive indexes of CTAB and PC caps are 1.414 and 1.40, respectively, which will create a blue shift of 13.7 nm for GNRs with aspect ratio 4.5; experimentally we observed a blue shift of 15 nm (from 847 to 832 nm), as shown in Figure 3.

Compared to PC activation, AMATZ and MUDA activation are both more effective; over 90% of GNRs could be recovered after the activation procedure. Figure 4a shows the AMATZ activation for GNRs with aspect ratio 3.5; Figure 4b shows the MUDA activation for GNRs with aspect ratio 2. The intensity changes of the plasmon bands are trivial compared to the PC procedure, indicating a much higher GNR recovery. The refractive index for AMATZ is unknown, and for MUDA, ($n = 1.463$[35]), the effective refractive index was calculated. Although $n_{\text{MUDA}} > n_{\text{CTAB}}$, because MUDA forms a monolayer, $d_{\text{MUDA}} = 1.69$ nm,[35] which is much smaller than d_{CTAB}; the effective refractive index of the MUDA cap is 1.392, smaller than that of the CTAB cap (1.414). For GNRs with aspect ratio 2, a blue shift of 10.3 nm is expected, which matched well with the experimental value of 11.5 nm.

To further confirm the surface chemistry modification of the AMTAZ step, where quantitative analysis of the GNR spectral response is not possible without refractive index data on AMTAZ, Raman microspectroscopy was utilized. A droplet of 0.1 M CTAB aqueous solution and 10 mM AMTAZ aqueous solution was placed on a glass slide and allowed to dry to form a thin layer of CTAB and AMTAZ on the glass surface. A Bruker Senterra Raman microscope (Bruker Optics, Inc., Billerica, MA) with 785 nm excitation laser at 25 mW was used to measure the Raman spectra of CTAB and AMTAZ. The Raman spectra of gold nanorods with CTAB cap and gold nanorods with AMTAZ cap were also measured using the same settings. Ten spectra were acquired for each sample type and averaged to yield a final spectrum as presented in Figure 5.

Results in Figure 5 depict the surface enhanced Raman scattering (SERS) effect due to its intense spectral signals. In order to compare the SERS spectra of the nanorods to the spectra of the pure chemicals, all spectra were normalized. The CTAB-capped gold nanorods display characteristic CTAB Raman bands at 455, 763, 1061, 1127, 1295, and 1460 cm^{-1}. After AMTAZ activation, the gold nanorods display characteristic AMTAZ Raman bands at 479, 1064, 1425, and 1478 cm^{-1}. The strong CTAB characteristic bands at 455, 1127, and 1460 cm^{-1} disappear

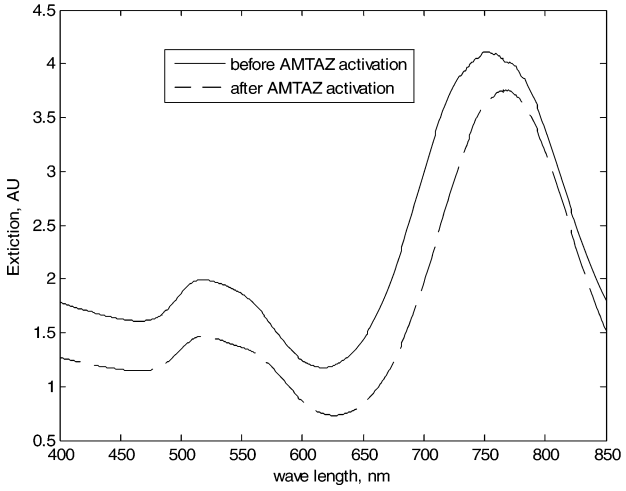

(a)

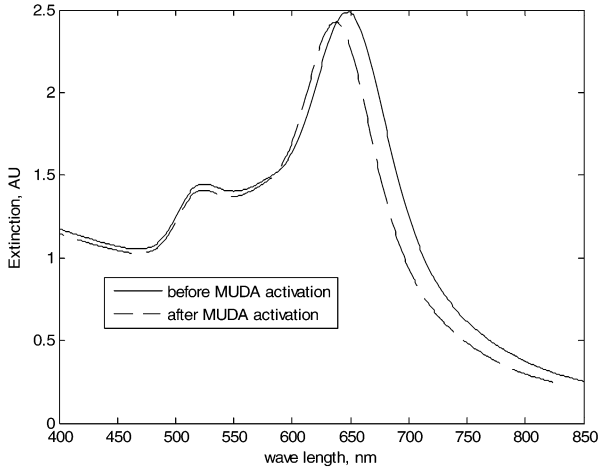

(b)

Figure 4. Plasmon spectra of GNRs before/after (a) AMTAZ and (b) MUDA activation.

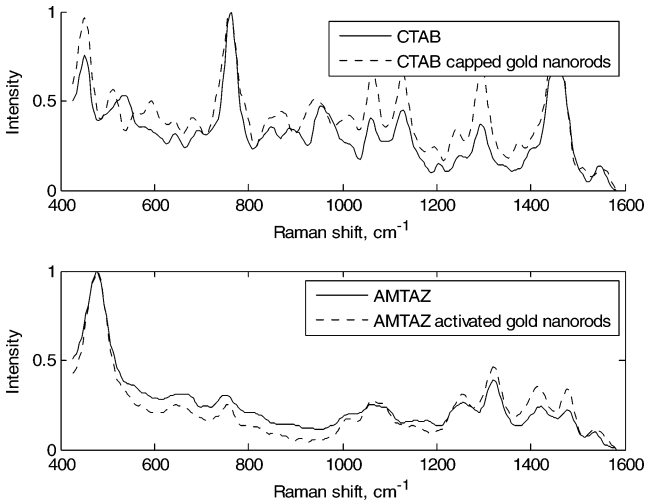

Figure 5. Raman spectra of CTAB-, AMTAZ-, and CTAB-capped gold nanorods and AMTAZ-activated gold nanorods.

altogether. This observation confirms that the CTAB cap is completely replaced by the AMTAZ cap, and the residual CTAB on the gold nanorod surfaces is negligible.

A cytotoxicity study was subsequently conducted to investigate the effect of the PC-, AMTAZ-, and MUDA-capped GNRs on

(35) Haes, A.; van Duyne, R. P. *J. Am. Chem. Soc.* **2002**, *124*, 10596−10604.
(36) Murphy, C. J.; Sau, T. K.; Gole, A. M.; Orendorff, C. J.; Gao, J.; Gou, L.; Hunyadi, S. E.; Li, T. *J. Phys. Chem. B* **2005**, *109*, 13857−13870.
(37) Ardhammar, M.; Lincoln, P.; Nordén, B. *Proc. Natl. Acad. Sci. U.S.A.* **2002**, *99*, 15313−15317.

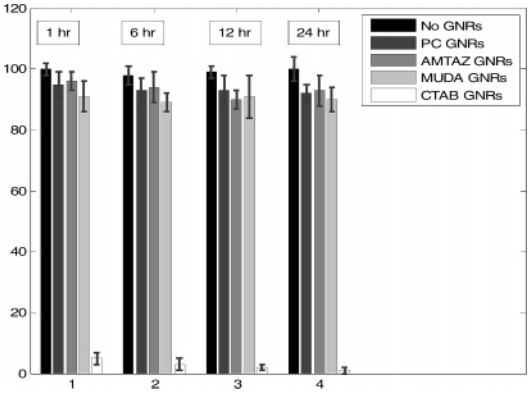

Figure 6. Viability of cells incubated with GNRs with PC, AMTAZ, MUDA, and CTAB capping after 1, 6, 12, and 24 h.

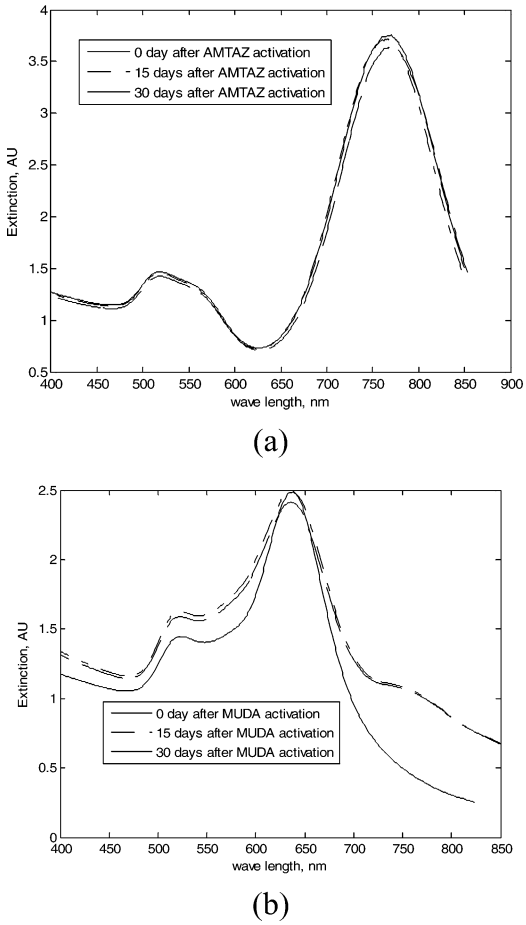

Figure 7. Stability of (a) AMTAZ- and (b) MUDA-capped GNRs.

MCF 10A, a human breast epithelial cell line. Cells with no GNRs were used as control and compared with (i) CTAB-, (ii) PC-, (iii) AMTAZ-, and (iv) MUDA-capped GNRs. The original CTAB-capped GNRs were subjected to two rounds of centrifugation to remove the extra CTABs in the solution. A 1 mL portion of cell culture with cell concentration of 1.45×10^6/mL was placed in each well. Two wells each were incubated with 20 μL of PBS buffer, 20 μL of CTAB-capped GNRs (aspect ratio 5.5, 0.25 mM as Au atoms), 20 μL of PC-capped GNRs (aspect ratio 4.5, 0.25 mM as Au atoms), 20-μL of AMTAZ-capped GNRs (aspect ratio 3.5, 0.25 mM as Au atoms), and 20 μL of MUDA-capped GNRs (aspect ratio 3.5, 0.25 mM as Au atoms). The viability of the cells was evaluated by Trypan blue staining. Figure 6 shows the viability of cells after 1, 6, 12, and 24 h of incubation (% of cells alive). It is clearly shown that CTAB-capped GNRs are highly toxic, even after two rounds of centrifugation; PC-, AMTAZ-, and MUDA-capped GNRs are much less toxic to the cells: 90% or more of cells are still viable after 24 h of incubation with these GNRs.

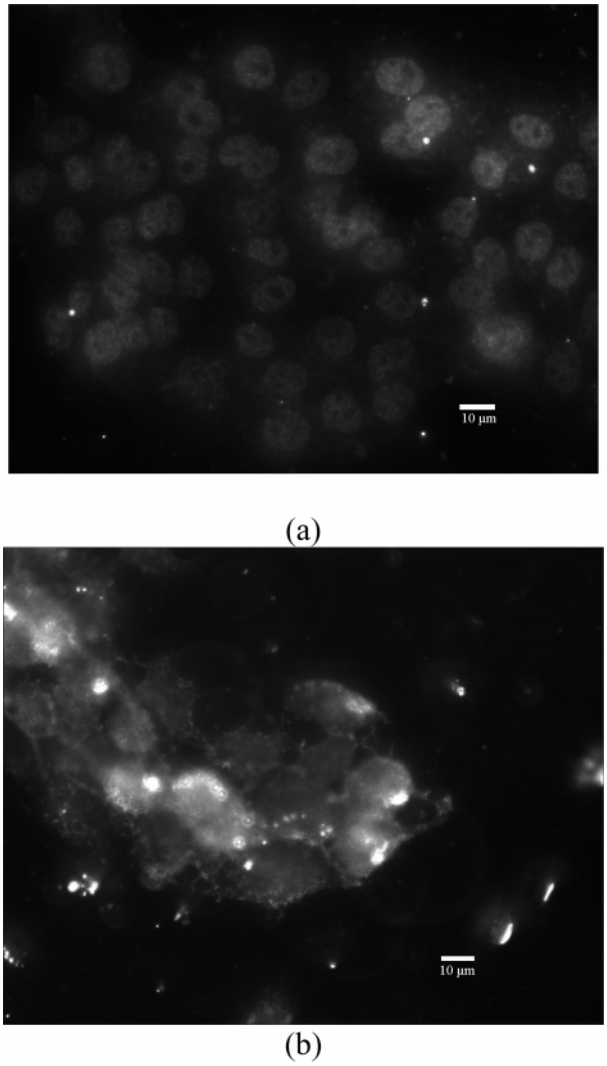

Figure 8. Dark field microscopic images of MCF10A CD44+ cells: (a) cells without GNrMPs attached and (b) cells with GNrMPs attached.

The stability of the AMTAZ- and MUDA-capped GNRs in PBS buffer solution was monitored over a 30-day period. The plasmon spectra of the nanorods at 0, 15, and 30 days after activation are shown in Figure 7a,b. No significant changes due to aggregation were observed for the AMTAZ-capped GNRs, suggesting that the stability of the AMTAZ-capped GNRs is satisfactory. For MUDA-capped GNRs, an interesting observation noted was the appearance of a broad band at 770 nm, which could be attributed to the "head-to-tail" connection of GNRs caused by hydrogen-bond formation between the MUDAs on different nanorods, consistent with earlier reports.[31]

Further functionalization of the AMTAZ-capped GNRs with anti-CD44 antibodies was conducted, and CD44 gold nanorod molecular probes (GNrMPs) were produced. Preselected CD44+ MCF10A cells were incubated with the CD44 GNrMPs and with nonfunctionalized GNRs for 30 min and repeatedly washed with PBS buffer. Figure 8 shows the dark field microscopic images of preselected CD44+ MCF10A cells with CD44 GNrMPs and nonfunctionalized GNRs. The attachment of the GNrMPs to the cell surface CD44 receptors is clearly demonstrated, suggesting that the functional molecular probes were successfully fabricated

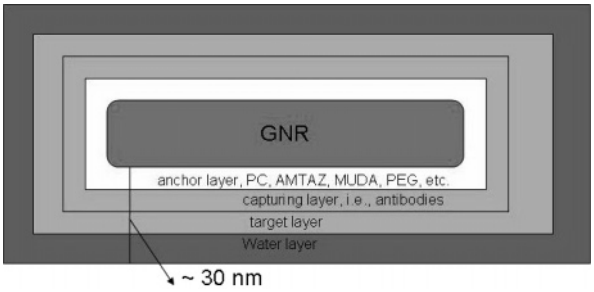

Figure 9. Microenvironment surrounding a GNrMP.

using the AMTAZ-capped gold nanorods. It should be noted that when the nonfunctionalized GNRs were incubated with cells for a long time (over night), eventually they are uptaken by the cells through endocytosis. The very short duration of the incubation time and multiple washing steps ensured that there were no GNRs inside or around the cells. Given the fact that different nanorod molecular probes can be easily distinguished by their unique plasmon spectra, these nanorod molecular probes can be used to monitor multiple cell surface biomarkers simultaneously.

The sensitivity of GNrMPs to molecular binding events is determined by the microenvironment in the vicinity and the aspect ratio of GNRs. The microenvironment of a GNR is illustrated in Figure 9. For GNRs with the same aspect ratio, the thickness of the anchor layer is negatively correlated to the sensitivity of the GNrMPs to molecular binding events. As discussed earlier, CTAB/PC-capped GNRs have similar anchor layer structure (bilayer) and thickness (5−6 nm), suggesting similar response to sensitivity to molecular binding events; AMTAZ- and MUDA-capped GNRs contain a monolayer as their anchor layer; hence, their sensitivity to molecular binding events should be higher. Another factor is that for CTAB/PC-capped GNRs, antibodies are physisorbed onto the GNRs, and the attachment is less robust than the antibody immobilization protocol adopted for the AMTAZ/MUDA-capped GNRs, which has a covalent bond. Hence, fewer antibodies molecules bind to each CTAB/PC-terminated GNR on average, which will further reduce the sensitivity of the GNrMPs to their molecular targets. The sensitivity of the GNrMPs is directly measured by the red-shift of the longitudinal plasmon band of the GNrMPs upon target binding. In this study, we investigated two different GNrMPs prepared from GNRs with aspect ratio 3.0 and 4.5, respectively. Rabbit anti-mouse IgGs were used as capturing agents and mouse IgGs were used as targets. Two target concentrations were selected, one at 1 μM, which is high enough to saturate all GNrMPs, hence rendering the maximum response signal, and the other is 10 nM, which is close to the detection limits of these GNrMPs. The results are shown in Figure 10 and Table 1. It can thus be confirmed that CTAB- and PC-capped GNrMPs show comparable sensitivity, which is considerably lower than that of AMTAZ/MUDA-capped GNRs; CTAB/PC GNrMPs of aspect ratio 3.0 cannot detect the presence of target at 10 nM, whereas AMTAZ/MUDA GNrMPs yield good results; the maximum signals produced by AMTAZ/MUDA GNrMPs are consistently

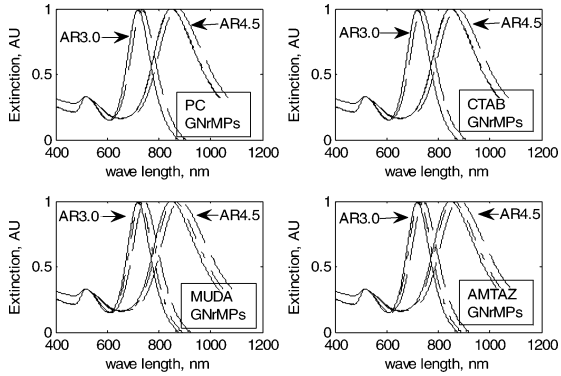

Figure 10. Sensitivity of GNrMPs made from PC-, CTAB-, MUDA-, and AMTAZ-terminated GNRs, as indicated by the red-shift of the longitudinal band induced by target binding at two different concentrations, 1 μM and 10 nM.

Table 1. Sensitivity of Molecular Probes Made from GNRs[a]

	GNR aspect ratio 3.0		GNR aspect ratio 4.5	
GNR cap	[T] = 1 μM	[T] = 10 nM	[T] = 1 μM	[T] = 10 nM
CTAB	16	n/a	23	2.5
PC	14.5	n/a	21.5	2
AMTAZ	22.5	6.5	32	10
MUDA	24	7	32.5	11.5

[a] Sensitivity is measured by the red-shift in nanometers of the longitudinal band upon target binding. n/a means no red-shift was detected.

higher than that of CTAB/PC GNrMPs. It is clearly shown that the AMTAZ- and MUDA-terminated GNRs are preferred for sensing molecular binding studies. Although thiolated PEG activation was not studied in this work, given the size of the PEG molecules, it is reasonable to hypothesize that the PEG-terminated GNRs will not be as sensitive compared to the former demonstrations of molecular binding events.

Conclusion

In this paper, we report a novel procedure for effective replacement of the CTAB cap on gold nanorods with biocompatible and functionalization-friendly small organothiols (AMTAZ and MUDA). The procedure is flexible and allows selection of application-dependent organothiols. The organothiol-capped GNRs were also very stable. The cytotoxicity of both AMTAZ- and MUDA-capped gold nanorods was shown to be negligible, at 0.25 mM. The organothiol-activated gold nanorods can be easily functionalized with antibodies to fabricate molecular probes. The sensitivity of molecular probes made from organothiol-activated GNRs is higher than CTAB/PC-terminated GNRs. The proposed protocol can be utilized to further functionalize the nanorods to tether DNA/RNA, enzymes, and proteins to monitor interactions in living cells as well as for in vivo diagnostics.

LA701111E